



Investigation of flux attenuation and crystallization behavior in submerged vacuum membrane distillation (SVMD) for SWRO brine concentration

Tong Zou^{a,b}, Guodong Kang^{a,*}, Meiqing Zhou^a, Meng Li^a, Yiming Cao^{a,*}

^a Dalian National Laboratory for Clean Energy (DNL), Dalian Institute of Chemical Physics, Chinese Academy of Sciences, Dalian 116023, China

^b University of Chinese Academy of Sciences, Beijing 100049, China

ARTICLE INFO

Keywords:

Submerged vacuum membrane distillation
Concentration process
Flux attenuation
Crystallization behavior

ABSTRACT

This work studied the concentration of seawater reverse osmosis (SWRO) brine by a submerged vacuum membrane distillation (SVMD) process. Factors for flux attenuation including CaSO_4 crystallization, vapour pressure depression, the increase of heat transfer resistance and membrane fouling were distinguished by the combination of experiment and theoretical calculation. It was suggested that CaSO_4 crystallization was the main reason for flux attenuation, which should be eliminated by appropriate feed pretreatment with additional of Na_2CO_3 and HCl. The combined effect of other three factors was another important reason for flux attenuation. Although the effect of CaSO_4 crystallization was eliminated, there still existed a critical VCF after which membrane fouling and increase of heat transfer resistance could not be neglected. The result indicated that this critical VCF was about 2.5 under the experimental condition, which was far less than the VCF at which NaCl solution reached saturation. Therefore, finding an effective method to mitigate membrane fouling was still necessary. It was concluded that decreasing the concentration rate by changing the operation mode could effectively increase the critical VCF to 3.7. Meanwhile, the crystallization behavior of NaCl and the size and quality of crystal products would be affected.

1. Introduction

Freshwater shortage is an increasingly problem all over the world since only 1% of the water on the earth is available for human to drink [1]. Seawater desalination is now feasible to produce large quantities of high-quality freshwater technically and economically. Reverse osmosis (RO), known as one of the most energy efficient desalination technologies, accounts for more than 60% of the global desalination capacity [2]. However, the concentration of NaCl in seawater is 3.0–4.5%. Considering the recovery rate of RO process is 30–50%, then the osmotic pressure of the concentrated brine is as high as 35–74 bar [3]. If the recovery rate is further improved, the osmotic pressure that needs to be overcome is even higher. Obviously, RO is not suitable for this purpose.

Membrane distillation (MD) is a thermal-based membrane separation process which is known since 1963 [4]. The driving force in MD process is the vapour pressure difference across the hydrophobic membrane rather than the applied absolute pressure difference. As such, one of the greatest advantages of MD over RO is that it shows great potential in treating high salinity brine without the limitation of the osmotic pressure [5–7]. In addition, since the non-volatile

components in the feed solution can not pass through the membrane pores in the form of vapour molecules, the rejection rate of salt is closed to 100% theoretically.

A significant bottleneck existed in MD process is the flux attenuation with time [8]. In most cases, drastic flux decline which has a significant effect on MD performance is attributed to membrane fouling or crystallization [9,10]. As a result, most of the presented researches on MD have focused on the investigation of membrane fouling and its controlling measures. For example, P. Zhang et al. pointed out that in the process of treating SWRO brine using direct contact membrane distillation (DMCD), the reduction of flux was primarily caused by precipitation of CaSO_4 and CaCO_3 [11]. Q.M. Nguyen et al. also investigated the fouling development in DCMD process at different degrees of SWRO brine concentration [12]. J.A. Sanmartino et al. discussed the effect of different chemical pretreatment strategies on scale reduction [13]. However, in addition to membrane fouling or crystallization, reasons for flux decline also include water vapour depression of saline brine [14] and the increase of heat and mass transfer resistance due to the temperature and concentration polarization [15,16], which have little effect on MD performance but are inevitable. In terms of seawater reverse osmosis (SWRO) brine, reasons for flux attenuation

* Corresponding authors.

E-mail addresses: kanguod@dicp.ac.cn (G. Kang), ymcao@dicp.ac.cn (Y. Cao).

<https://doi.org/10.1016/j.cep.2019.107567>

Received 1 April 2019; Received in revised form 17 June 2019; Accepted 19 June 2019

Available online 08 July 2019

0255-2701/ © 2019 Elsevier B.V. All rights reserved.

Nomenclature

A	Effective area of membrane outer surface (m ²)
J	Permeate flux (kg m ² h ⁻¹)
K _m	Membrane distillation coefficient (kg m ⁻² s ⁻¹ Pa ⁻¹)
M	Molecular weight of water (kg mol ⁻¹)
m	The weight of permeate (kg)
P _{fm}	The pure water vapor pressure at membrane surface(Pa)
P _v	Pressure at the vacuum side (Pa)

R	Universal gas constant (J mol K ⁻¹)
T _f	Temperature of solution in the feed bulk (K)
T _{fm}	Temperature of solution at membrane surface(K)
t	Operation time (h)
r	Mean pore size of membrane (m)
ε	Membrane porosity
σ	Membrane thickness (m)
τ	Membrane tortuosity
C	Mole fraction of NaCl in solution

with time are often the combination of above factors on account of the complexity of its components, but it tends to get confused and lack of further study. The combination of experiment and MD model is an effective method to further analyze reasons for flux attenuation. There are several literature reports performing heat and mass transfer modeling on traditional homogeneous membrane [17,18] and supported membranes [19–21] mathematically, all of which has significant scientific insights and reference effect.

Based on the above consideration, the simulated SWRO brine was used as the object of this study. Reasons for flux attenuation in a submerged vacuum membrane distillation (SVMD) concentration process were investigated systematically. Firstly, the effect of membrane fouling caused by the insoluble component CaSO₄ on flux attenuation was illustrated separately and an appropriate feed pretreatment method was determined to eliminate the influence of CaSO₄ crystallization. On this basis, the specific reason for flux decline in SVMD process for SWRO brine concentration was analyzed in detail by combining the experiment and theoretical calculation. Factors such as water vapour depression of saline brine, the increase of heat transfer resistance and membrane fouling were distinguished in this study and the influence of the latter two factors on concentration process was weakened by changing the operation mode. Meanwhile, the crystallization behavior of NaCl in this process was also investigated.

2. Theory

In vacuum membrane distillation (VMD), a linear relationship between the permeate flux J and the transmembrane pressure difference of water vapour can be written as Eq. (1) [22]. The influence of non-condensable gases to the mass transfer inside membrane pores is negligible [23].

$$J = k_m [P(P_{fm}, c) - P_v] \quad (1)$$

Where P_v is the pressure in the vacuum side. k_m is the membrane distillation coefficient, which can be written as Eq. (2) when only Knudsen diffusion is considered [6].

$$k_m = 1.064 \frac{r\varepsilon}{\tau\delta} \sqrt{\frac{M}{RT_{fm}}} \quad (2)$$

Where r , ε , τ , σ is the mean pore size, porosity, tortuosity and membrane thickness, respectively. M is the molecular weight of water and R is the gas constant.

The vapour pressure of saline water $P(P_{fm}, c)$ is represented as a product of vapour pressure of pure water P_{fm} and a weighting function of $f(C)$ of saline concentration [14]:

$$P(P_{fm}, c) = P_{fm} f(C) \quad (3)$$

Where $f(C)$ should satisfy the following relationship:

$$f(C \rightarrow 0) = 1 \quad (4)$$

Take NaCl solution for example, the relationship of saline concentration and the $f(C)$ can be written as [5]:

$$f(C) = (1 - C)(1 - 0.5C - 10C^2) \quad (5)$$

Where C is mole fraction of NaCl in feed solution. Other empirical relationships can be found in an excellent review [24]. The pure water vapour pressure P_{fm} is given by the Antoine's equation [18]:

$$P_{fm} = \exp\left(23.1964 - \frac{3816.44}{T_{fm} - 46.13}\right) \quad (6)$$

Where T_{fm} is the membrane surface temperature in the feed solution.

3. Experimental

3.1. Feed solution

The composition and content of minerals in SWRO brine were referred to the previous literature [25]. According to different researching purposes and needs, two simulated SWRO brines with different concentration were used as feed solution, named as SWRO-1 and SWRO-2. The composition, concentration, pH and conductivity of the feed solution were listed in Table 1. All chemicals needed were purchased from Tianjin Kemiou Chemical Reagent Company.

3.2. Chemical pretreatment of feed solution

According to the chemical composition of the simulated feed solution, following methods were considered as chemical pretreatment:

3.2.1. Addition of Na₂CO₃

It seems to be one of the simplest chemical pretreatment method. CO₃²⁻ introduced to the system reacts with Ca²⁺ to form CaCO₃ and the formation of CaSO₄ is avoided effectively [13]. In this experiment, a certain amount of Na₂CO₃ was added to the feed solution according to stoichiometric coefficient. The excess amount of Na₂CO₃ was about 20–30%. Then the feed solution was stirred at 75°C for 45–60 min, followed by filtration process in order to remove CaSO₄ precipitation from the feed solution.

3.2.2. Addition of Na₂CO₃ and HCl

In order not to introduce the additional CO₃²⁻, the first method was improved as follows: After pretreatment with the method mentioned above, a certain amount of 6 mol/L HCl was also added to the feed solution to turn the excess CO₃²⁻ into CO₂ and H₂O. The pH of the feed solution was adjusted to about 6.0–6.5.

3.3. Membrane and membrane module used in SVMD

The parameters of PTFE membrane and membrane module used in SVMD were listed in Table 2.

Table 1

The composition, concentration, pH and conductivity of feed solution.

	NaCl (mg/L)	KCl (mg/L)	MgCl ₂ (mg/L)	MgSO ₄ (mg/L)	CaSO ₄ (mg/L)	pH	Conductivity (mS/cm)
SWRO-1	36200	1000	4500	2900	1800	7.0-7.5	85-90
SWRO-2	65,500	1500	6900	2900	1800	7.0-7.5	144-155

Table 2
The parameters of PTFE membrane and membrane module.

PTFE hollow fiber membrane	
Outer diameter(mm)	1.7
Inner diameter (mm)	0.8
Wall thickness (μm)	450
Porosity (%)	41.0
Tortuosity	2.6
Mean pore size (μm)	0.186
LEP _w (bar)	3.1
Membrane module for SVMDC	
Effective length of membranes(cm)	50
No. of PTFE hollow fibers	6
Effective area of membranes (m ²)	0.016

3.3.1. Preparation of PTFE hollow fiber membrane

As a crystalline polymer, PTFE is considered to be an ideal material for MD process compared with PVDF and PP [26–28] due to its superior hydrophobicity, thermal stability, chemical resistance and mechanical strength [26,29]. In this study, self-made PTFE hollow fiber membrane was used. The preparation method included mixing and aging, billet preforming, extrusion, stretching and sintering, which was described detailedly in our previous work [30,31]. The characterization methods of membrane properties such as porosity, tortuosity, mean pore size and liquid entry pressure (LEP_w) were described in elsewhere [32–35].

3.3.2. Membrane module used in S-VMDC

Six PTFE hollow fiber membranes were folded together to fabricate a “U-shaped” membrane module using an epoxy resin to seal at one end. The effective length of each hollow fiber was 50 cm. The module could be reused by simple water cleaning and it was proved that this module showed stable performance and no wetting phenomenon occurred during the experiment.

3.4. Submerged vacuum membrane distillation (SVMDC)

The experimental set-up of the SVMDC is illustrated in Fig.1. The “U-shaped” PTFE hollow fiber membrane module was submerged in a constant temperature feed tank. The outer surface of the membrane was contacted with hot feed solution directly. The feed solution was heated by a thermostatic magnetic stirring apparatus. The feed temperature was maintained at 75°C throughout tests, which was controlled by a temperature transmitter. In order to improve the heat and mass transfer

of boundary layer, the feed solution was stirred at 1350 rpm by a magnetic rotor. The vacuum pressure of the permeate side was controlled at –85 kPa using a water circulating multi-purpose vacuum pump which was connected to a pressure transmitter. The positive and negative error was controlled within 1.0 kPa. Both the temperature transmitter and pressure transmitter were directly connected to the PLC so that the feed solution temperature and vacuum pressure of the permeate side could be monitored in real time during the whole experiment. The water vapour passed through the membrane pores was condensed in a condenser and collected by a permeate tank. The weight of the permeate was measured every 30–60 minutes by an electronic balance. The permeate flux J was calculated using the following equation:

$$J = \frac{m}{A \cdot t} \quad (7)$$

where, m is the weight of permeate, A is the effective area of membranes and t is the operation time.

In order to make a intuitive comparison of experimental results, all the flux data were presented in terms of normalized flux ratio J/J_0 [36]. J_0 was obtained when the deionized (DI) water was used as feed at the same operating condition without stirring.

The permeate quality was continuously monitored by a conductivity meter. Salt rejection was calculated using the following equation:

$$R[\%] = \frac{C_f - C_p}{C_f} \times 100 \quad (8)$$

where, C_f and C_p is the conductivity of the feed and permeate, respectively.

The concentration degree was expressed in terms of volume concentration factor (VCF). The calculation method of VCF depended on the operation mode during the concentration process. In the first operation mode, no feed solution was replenished to the feed tank and the liquid level declined during the concentration process, the VCF was calculated as Eq(9):

$$VCF = \frac{V_{initial}}{V_{initial} - V_{total,permeate}} \quad (9)$$

In the second operation mode, the liquid level remained constant and then the concentration rate was decreased by continuously feeding the feed solution at the same rate of produced fresh water, the VCF was calculated as follows [37]:

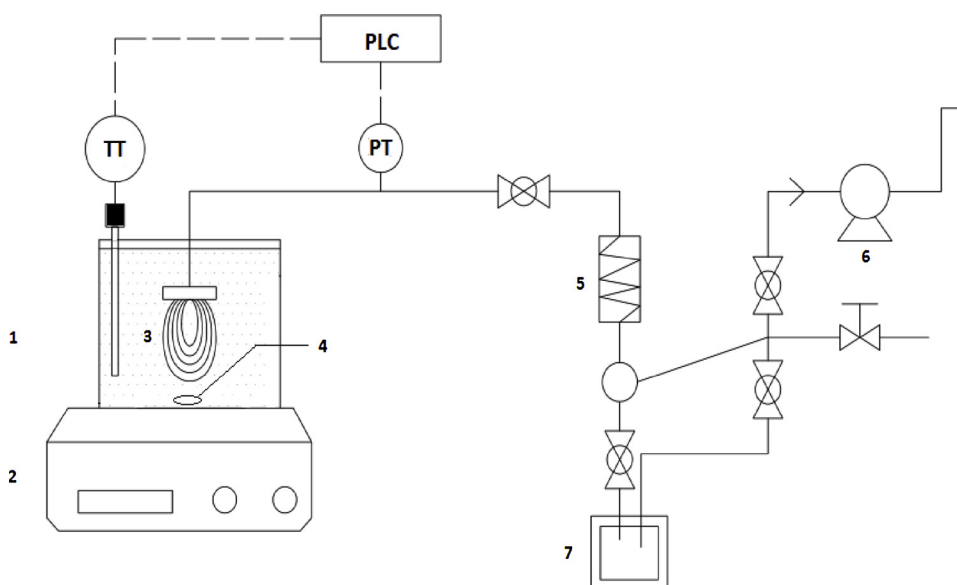


Fig. 1. Schematic of the SVMDC setup.

1. Constant temperature feed tank
 2. Thermostatic magnetic stirring apparatus
 3. “U-shaped” PTFE hollow fiber membrane module
 4. Magnetic rotor
 5. Condenser
 6. Water circulating multi-purpose vacuum pump
 7. Permeate tank
- *PLC: Programmable Logic Controller
TT: Temperature Transmitter
PT: Pressure Transmitter

$$VCF = \frac{V_{\text{initial}} + V_{\text{total,permeate}}}{V_{\text{initial}}} \quad (10)$$

where V_{initial} is the initial volume of feed solution and $V_{\text{total,permeate}}$ is the total amount of fresh water produced.

At the completion of the concentration process, the bulk solution was static cooled down to room temperature, then filtered by a filter paper and dried in a 100°C oven to constant weight. NaCl crystals were obtained in this way and their macroscopic and microscopic forms were observed by naked eye and Environmental Scanning Electron microscope (ESEM) respectively.

4. Results and discussion

4.1. Effect of CaSO_4 fouling and scaling on the flux attenuation

Of all the components in the feed solution used in this experiment, CaSO_4 has the lowest solubility which shows the highest tendency to fouling and scaling. To highlight the effect of CaSO_4 on the flux attenuation, SWRO-1 was used as feed solution to avoid the influence of NaCl crystallization. The concentration process was operated under the second operation mode. According to previous publications, it was indicated that CaSO_4 crystallization has a certain induction time [38]. The initial idea was to “reset” the induction time by intermittent membrane cleaning and feed solution filtration. Therefore, every time when J/J_0 decreased below 0.6, membrane module was taken out for cleaning and feed solution was filtered for removing the CaSO_4 crystals.

The normalized flux and permeate conductivity as the function of VCF were presented in Fig. 2. It showed that in the first cycle, the normalized flux was always kept above 0.8 when VCF was less than 3.3. While after VCF exceeded 3.3, the normalized flux rapidly dropped from 0.87 to 0.61 within only 150 min. It was clear that the rapidly flux decline was attributed to the crystallization of CaSO_4 when its concentration in feed solution reached the saturation point, which was illustrated detailedly by many other publications [38–40]. It was interesting to note that although the normalized flux could be recovered to the previous level after every cleaning and filtration, the flux decline rate became more and more rapidly. On one hand, the ionic strength in feed solution increased with the increase of VCF, leading to the decrease of CaSO_4 solubility [8], which made it easier for CaSO_4 to crystallize. On the other hand, membrane cleaning and feed solution filtration could only remove the visible CaSO_4 crystals already formed, while the dissolved CaSO_4 in feed solution was still in metastable state. Slight changes in external condition could promote the formation of CaSO_4 crystals. It implied that the operation time of each cycle was becoming shorter and shorter. In the fourth cycle, the whole concentration process lasted only 330 min. The final VCF in this experiment was 5.3, while the concentration of NaCl was far below its limiting saturation concentration.

From the perspective of application, it is too impractical to clean the membrane module and filter the feed solution so frequently. The above experimental result proved the infeasibility of intermittent membrane cleaning and feed filtration. As a result, it is particularly important to remove CaSO_4 completely through feed solution pretreatment before the SVMD process, which will be discussed in detail in the following section.

4.2. The effectiveness of feed solution pretreatment

The most straightforward idea is completely converting the SO_4^{2-} existing in feed solution into CO_3^{2-} which has the lower solubility and removing the carbonate by filtration before the SVMD test. The detailed information was described in Section 3.2.1. In order to investigate the effectiveness of pretreatment, the SVMD test used SWRO-1 as feed solution and was carried out after pretreatment. The result was also compared with that without pretreatment, which was shown in Table 3.

Contrary to the expectation, the VCF_{critical} decreased from 3.1 to 1.7 after feed pretreatment by Na_2CO_3 . In other words, it was suggested that the addition of Na_2CO_3 introduced the excessive CO_3^{2-} , which could not be entirely removed by filtration in the form of carbonate precipitation. During the concentration process, the concentration of both CO_3^{2-} and Mg^{2+} in feed solution increased gradually, making it easy to form the precipitation again. At the end of the experiment, it could be observed that the wall of feed tank was covered with a thin layer of sediment, which was insoluble in water but soluble in HCl. It further supported the above suggestion. Therefore, HCl was also introduced to remove the excess CO_3^{2-} , the detailed information was shown in Section 3.2.2. After pretreatment of feed solution by the second method, SVMD test was carried out for more than 30 h until VCF exceeded 5. Although the concentration of NaCl was not reached its saturation point at the end of the experiment, no precipitation was generated and the normalized flux did not show drastic decline during this concentration process, which proved that the second method was effective. For the following experiments, SWRO-2 was used as feed solution and was pretreated with the second method before SVMD test. This time, the concentration process was lasted until solution was saturated. CaSO_4 scaling and crystallization did not occur during the whole process, which further proved the effectiveness of feed pretreatment.

4.3. Submerged vacuum membrane distillation (SVMD) for SWRO brine concentration

4.3.1. Analysis of reasons for flux attenuation during the concentration process

SWRO-2 was used as feed solution for this concentration experiment. It was worth noting that the feed solution had been pretreated by the method mentioned above before SVMD test. Therefore, the effect of CaSO_4 crystallization on flux attenuation had been excluded. The first operation mode was adopted and the initial volume of the feed solution was 1000 mL. Both the experimental data and analysis result were compared with the SVMD concentration process of pure NaCl solution. (The initial concentration of pure NaCl was 65,500 mg/L)

For the concentration process of pure NaCl solution, as it was shown in Fig. 3, the normalized flux decreased gradually with the increase of VCF until the concentration of NaCl solution exceeded its limiting supersaturation level. According to the Eqs. (1), (3) and (6) in Section 2, if the effect of concentration polarization was not taken into consideration, the reasons for flux attenuation were as follows: Firstly, the increase of VCF led to the decrease of $f(C)$, which was inevitable for saline water. Secondly, it could be considered that the heat transfer resistance increased with the increase of VCF, resulting in the decrease of T_{fm} and

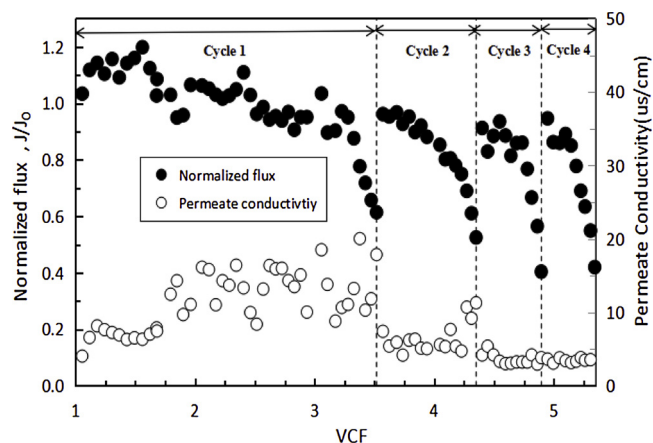


Fig. 2. The normalized flux and permeate conductivity as the function of VCF. J_0 was $6.9 \text{ kg/m}^2\text{h}$.

Table 3
The effect of feed solution pretreatment.

Pretreatment Method	VCF _{critical}
Without pretreatment	3.1
Addition of Na ₂ CO ₃	1.7
Addition of Na ₂ CO ₃ + HCl	-

*The VCF_{critical} was defined as the VCF at which the normalized flux began to drop significantly in a short time. The presence of VCF_{critical} signified that the membrane module had been suffered from fouling and scaling.

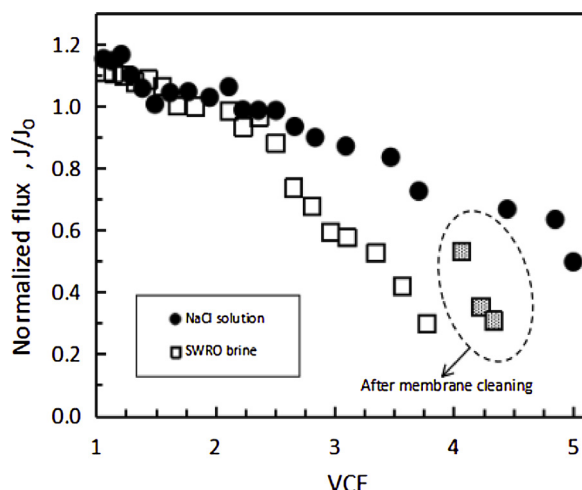


Fig. 3. The performance of SVMd for concentrating pure NaCl solution and SWRO brine. J_0 was 6.3 and 6.6 kg/m²h respectively.

thus affecting the driving force for mass transfer. Thirdly, if membrane fouling, surface crystallization or pore blocking occurred, the flux attenuation was probably related to the decrease of membrane distillation coefficient K_m due to the change of membrane structure parameters.

For further analysis of the specific reason for flux decline, the experimental data was plotted with $f(C)$ as x-axis and J/J_0 as y-axis, as shown in Fig. 4. For concentrating pure NaCl solution, J/J_0 and $f(C)$ presented obvious linear relationship, where $K_m \cdot P_{fm}/J_0$ was slope and $-K_m \cdot P_v/J_0$ was intercept, both of which have definite physical significance. The value of slope and intercept obtained by linear fitting were basically consistent with the result obtained by the theoretical calculation. This result indicated that during the whole process of concentrating pure NaCl solution to saturation state, the descent degree of permeate flux with the increase of VCF was always consistent with that of vapour pressure depression with the increase of VCF. As a result, it was reasonable believed that the flux decline could be attributed to the vapour pressure depression caused by the increase of feed concentration, while the effect of temperature polarization intensification and membrane fouling caused by pore blocking was almost negligible. It should be noted that phase separation took place only when VCF reached 5.0. Therefore, crystallization fouling of NaCl was not considered before that.

However, for the concentration process of SWRO brine, the performance of SVMd showed significantly different, as shown in Fig. 3. The flux decline rate increased prominently when VCF exceeded 2.5 comparing with that in pure NaCl solution. When VCF reached about 3.8, the normalized flux decreased to only 0.3. While the concentration of NaCl in feed solution was only about 249 g/L. Plotting the experimental data using the above method, as shown in Fig. 4, it was found that J/J_0 and $f(C)$ presented similar linear relationship when VCF was less than 2.5. While when VCF exceeded 2.5, the experimental data began to deviate from this linear relationship gradually. The greater VCF was, the larger deviation degree was. It was suggested that for

concentrating SWRO brine, the vapour pressure depression with the increase of VCF was no longer the only reason for flux decline after VCF exceeded 2.5. The increase of temperature polarization and the change of membrane structure parameters was more likely to be the reason for the further increase of flux decline rate.

In order to prove the above assumption, the experiment was paused and the membrane module was taken out for cleaning with deionized (DI) water when VCF reached 4. The aim of water cleaning was to recover the membrane structure parameters to the initial state, thus excluding the effect of membrane fouling. It was presented in Fig. 3 that the initial normalized flux could be recovered to a certain extent after water cleaning. Fig. 4 also showed that the distance between the first data after water cleaning and the linear relationship was shortened, but there still existed some differences. It signified that the increase of flux decline rate for concentrating SWRO brine was caused by both the increase of temperature polarization and the change of membrane structure parameters.

The different reasons of flux attenuation for concentrating pure NaCl solution and SWRO brine illustrated the effect of foreign ions on SVMd performance. First of all, comparing with pure NaCl solution, both the density and viscosity of SWRO brine were larger, leading to the increase of heat transfer resistance, thus the increase of temperature polarization. Secondly, since Mg^{2+} and OH^- existed simultaneously in feed solution, the risk of membrane fouling increased sharply.

4.3.2. Mitigating flux attenuation rate by changing the operation mode

In order to weaken the negative effect of foreign ions on SVMd performance and alleviate temperature polarization and membrane fouling, the second operation mode was adopted in this section. The most significant difference between the first and second operation mode was the relationship between the change of VCF over the operation time, which was illustrated in Fig. 5. The relationship between VCF and operation time was basically linear and concentration rate of the second operation mode was about two times lower than that of the first.

Fig. 6 showed the SVMd performance for concentrating SWRO brine with the second operation mode. The performance of the first operation mode was also presented in Fig. 6 as comparison. It could be seen from Fig. 6 that the operation mode had a significant impact on SVMd performance, especially when VCF exceeded 2.5. The permeate flux in the second operation mode was significantly higher than that in the first operation mode and the flux attenuation rate was also relatively slower. The experimental data in Fig. 6 was analyzed as the previous way to obtain the relationship between $f(C)$ and J/J_0 , as shown in Fig. 7. The dotted line was the linear relationship obtained during the pure NaCl concentration process. It was obviously showed that in the first

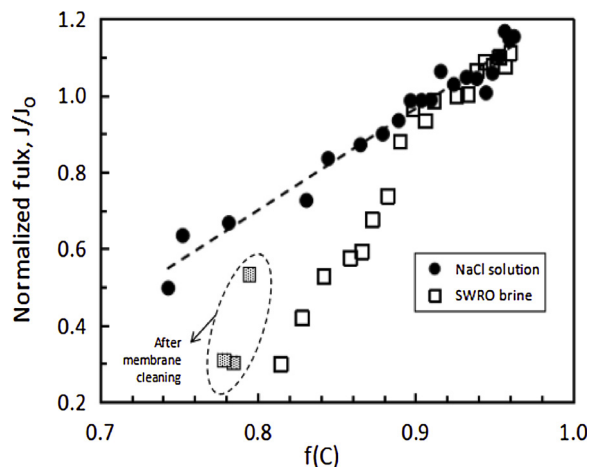


Fig. 4. The illustration of relationship between $f(C)$ and J/J_0 for concentrating pure NaCl solution and SWRO brine.

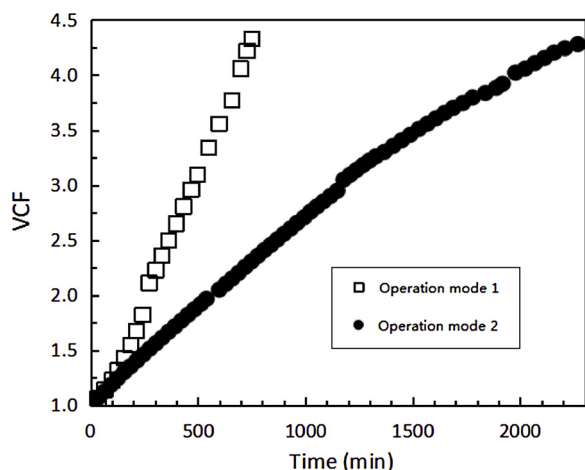


Fig. 5. The illustration of concentration rate in two operation modes.

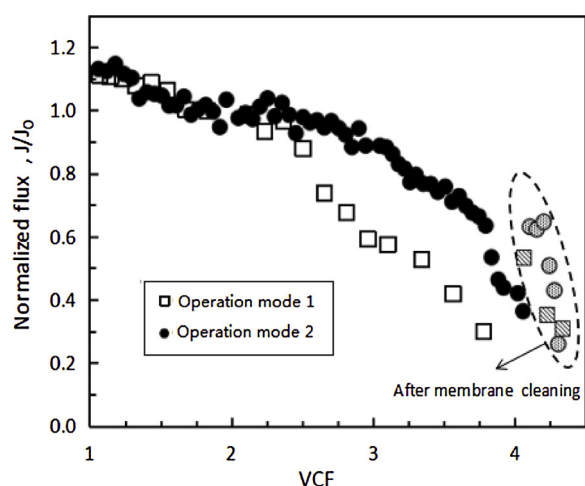


Fig. 6. The performance of SVMd for concentrating SWRO brine with different operation modes. J_0 was 6.4 and 6.6 kg/m²·h respectively for operation mode 1 and 2.

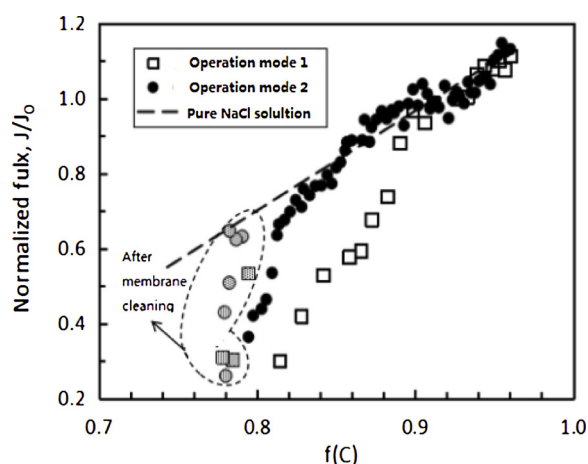


Fig. 7. The illustration of relationship between $f(C)$ and J/J_0 for concentrating SWRO brine with different operation modes.

operation mode, the experimental data deviated from this linear relationship very quickly when VCF was exceeded 2.5, while the experimental data was basically in the vicinity of this linear relationship until the VCF reached 3.7 in the second operation mode. It was indicated that decreasing concentration rate by changing the operation

mode could weaken the negative effect of foreign ions on SVMd performance, making the concentration process of SWRO brine more similar to that of pure NaCl solution. In terms of the second operation mode, the flux decline could be totally attributed to the decrease of vapour pressure depression with the increase of VCF when VCF was less than 3.7. After that, the change of membrane structure parameters and the increase of heat transfer resistance should also be considered as the reasons for flux decline.

In order to further analyze the specific reason for flux decline when VCF exceeded 3.7 in the second operation mode, the membrane module was also taken out for cleaning with deionized (DI) water. It was presented in Fig. 7. that the first three data after membrane cleaning was almost back to the dotted line. It could be reasonably inferred that the flux decline was almost due to the change of membrane structure parameters caused by fouling or pore blocking. While the influence of heat transfer resistance increase could be neglected in this case.

It could also observed in Fig. 7 that the last three data after membrane cleaning quickly deviated from the dotted line. It was also due to the change of membrane structure parameters, but the reason for variation of membrane structure parameters in this time was related to the crystallization of NaCl, which will discussed in detailed later.

4.3.3. NaCl crystallization behavior

Crystallization occurs when the feed solution is concentrated to a certain level where the concentration of NaCl exceeds its solubility. The reason for the phase transformation is the free energy of the initial solution phase is greater than the sum of the free energies of crystalline phase plus the final solution phase [41]. It is well known that the total free energy change during nucleation is the sum of surface free energy change and the volume free energy change [42]. The former is a positive term and the latter is a negative term. As a result, there is an intermediate size at which the total free energy change of the system is always decreased, which is known as the critical size [41]. In order to reach the critical size, a nucleation barrier must be overcome. Table 4 listed the critical VCF in SVMd process when observable phase separation took place in feed solution under different experimental conditions. It was found that for concentrating pure NaCl solution, observable phase separation took place when VCF was 5. While as for the concentration process of SWRO brine, the same phenomenon occurred when VCF was about 4.2. It probably due to the fact that the presence of other impurity ions in SWRO brine increased the instability of feed solution, thus reducing the nucleation barrier of NaCl. As a consequence, phase separation occurred with a relative lower VCF when comparing with that in pure NaCl solution. It was also worth noting that the change of operation mode could not have influence on the critical VCF.

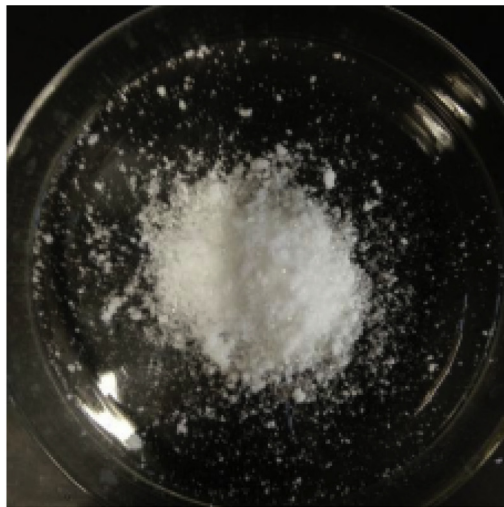
Fig. 8. showed the macroscopic and microscopic images of NaCl crystals obtained under different experimental conditions. These crystals presented different types of complexity due to primary or secondary agglomeration [43]. From both macroscopic and microscopic perspective, the existence of foreign ions greatly increased the particle size of NaCl crystals. Meanwhile, the quality of NaCl crystals were affected more or less. It was presented in Fig. 8 (b)-2 that a small amount of needlelike crystals could be observed in cubic NaCl crystals obtained

Table 4

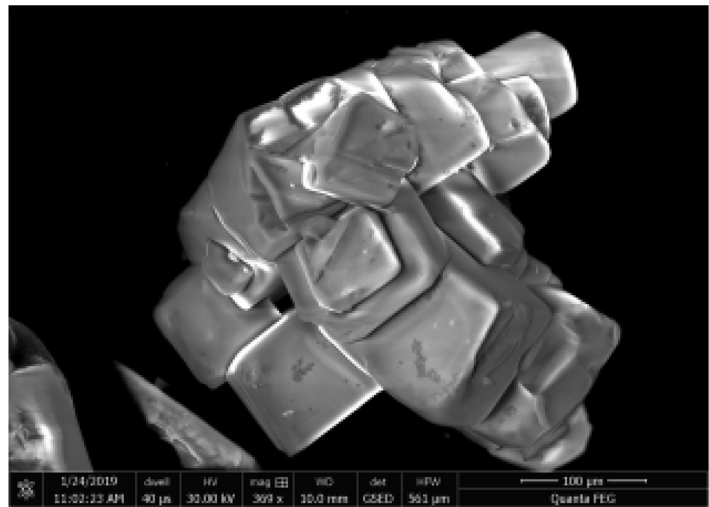
The critical VCF in SVMd process under different experimental conditions.

	VCF _{critical}
Pure NaCl solution	5.0
Simulated SWRO brine	
Operation mode 1	4.2
Operation mode 2	4.2

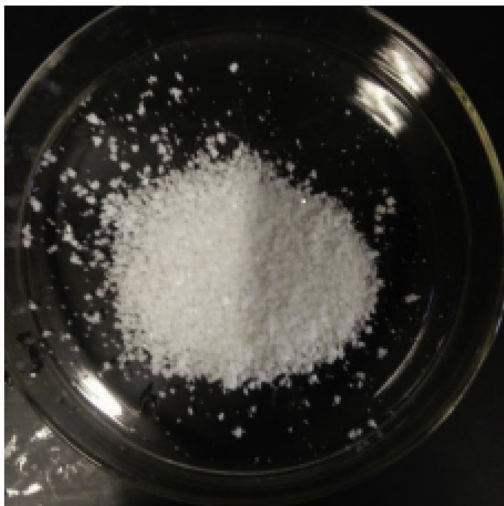
^aThe VCF_{critical} was defined as the VCF at which the observable phase separation took place in feed solution.



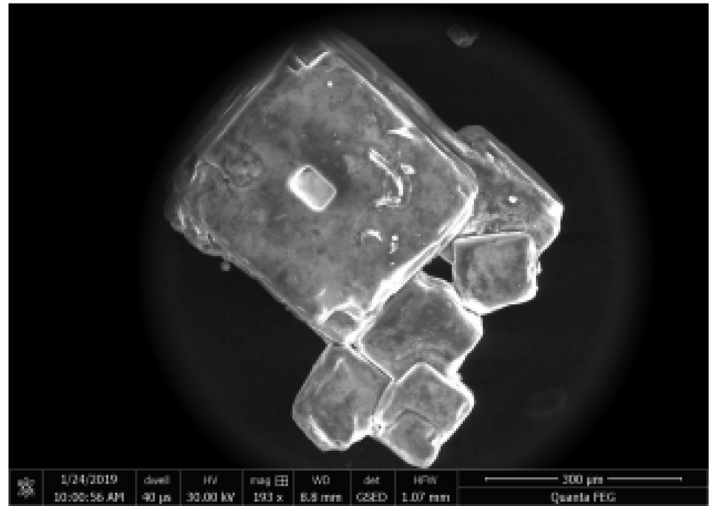
(a)-1



(a)-2



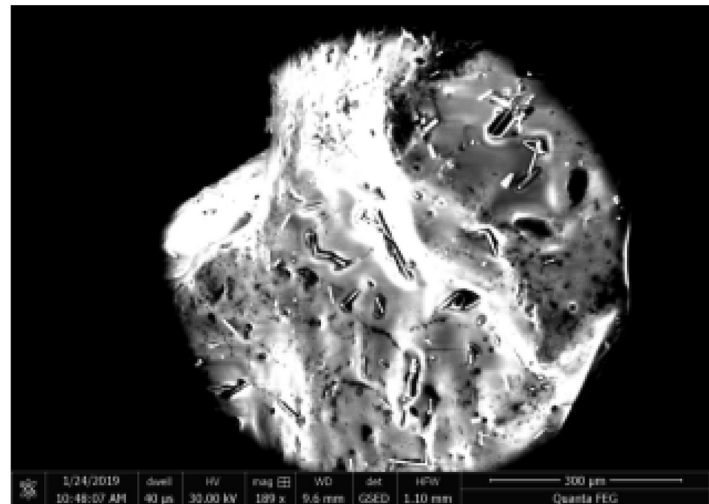
(b)-1



(b)-2



(c)-1



(c)-2

Fig. 8. Macroscopic (left) and microscopic (right) images of NaCl crystals obtained from concentrating (a) pure NaCl solution (b) SWRO brine with operation mode 1 and (c) SWRO brine with operation mode 2.

from SWRO brine with the first operation mode.

In addition, it was suggested that operation mode also had great influence on the thermodynamics and kinetics of crystallization behavior, leading to the differences in the size of NaCl crystals. Comparing with Fig.8(b)-2 and (c)-2, it was obviously seen that the size of NaCl crystals become much larger with the second operation mode. It is known to all that the supersaturation level produced during the concentration process needs to be eliminated by spontaneous nucleation and crystal growth. In the first operation mode, the concentration rate was relatively fast, the crystal surface in feed solution was insufficient, the crystal growth alone was not enough to eliminate the supersaturation level caused by water evaporation. Therefore, spontaneous nucleation occurred to consume the supersaturation level, leading to the formation of small size of NaCl particles (Fig.8 (b)-1, (b)-2). While in the second operation mode, the concentrate rate decreased, then the supersaturation level caused by water evaporation could be eliminated by crystal growth. As a result, larger size of NaCl crystals could be obtained in this case (Fig.8(c)-1 and (c)-2).

However, the quality of NaCl crystals were further affected with the second operation mode. It could be observed that a large numbers of needlelike crystals in Fig.8 (c)-2, which reduced the quality of NaCl crystals greatly. The reason for this phenomenon needed to be further study.

5. Conclusion

This study focused on the concentration of SWRO brine by using a submerged vacuum membrane distillation (SVMD) process. Reasons for flux attenuation included CaSO_4 crystallization, vapour pressure depression, heat transfer resistance and membrane fouling were distinguished by the combination of experiment and model calculation. NaCl crystallization behavior were also investigated. The conclusions were as follows:

- 1 CaSO_4 crystallization was the most important reason causing flux attenuation, which needed to be eliminated by appropriate feed pretreatment. Addition of Na_2CO_3 and HCl was proven to be effective.
- 2 The combined effect of vapour pressure depression, the increase of heat transfer resistance and membrane fouling was another important reason for flux attenuation. In the case of eliminating the effect of CaSO_4 crystallization, there still existed a critical VCF after which membrane fouling and increase of heat transfer resistance could not be neglected. The result indicated that this critical VCF was about 2.5 under the experimental condition, which was far less than the VCF at which NaCl solution reached saturation. Therefore, it was necessary to find an effective method to reduce the effect of the membrane fouling. It was suggested that decreasing the concentration rate by changing the operation mode could effectively increase the critical VCF to 3.7.
- 3 The presence of impurity ions reduced the nucleation barrier of NaCl, leading to the earlier phase transition. Meanwhile, the crystal size of NaCl increased while the quality decreased. With the decrease of concentration rate, the spontaneous nucleation of NaCl was inhibited and crystal growth played a dominated role, which resulted in a further increase of crystal size and a deterioration of crystal quality.

Acknowledgments

All the authors thank the financial support from Youth Innovation Promotion Association of the Chinese Academy of Sciences (No. 2016171) and Liaoning Revitalization Talents Program (XLYC1807240).

References

- [1] B.L. Pangarkar, M.G. Sane, M. Guddad, Reverse osmosis and membrane distillation for desalination of groundwater: a review, *Isrn Mater. Sci.* 2011 (2011) 2090–6080.
- [2] A. Deshmukh, et al., Membrane distillation at the water-energy Nexus: limits, opportunities, and challenges, *Energy Environ. Sci.* 11 (5) (2018).
- [3] S. Lee, et al., Hybrid desalination processes for beneficial use of reverse osmosis brine: current status and future prospects, *Desalination* (2018).
- [4] L. Camacho, et al., Advances in membrane distillation for water desalination and purification applications, *Water* 5 (1) (2013) 94–196.
- [5] Y. Yun, et al., Direct contact membrane distillation mechanism for high concentration NaCl solutions, *Desalination* 188 (1) (2006) 251–262.
- [6] J.P. Mericq, S. Laborie, C. Cabassud, Vacuum membrane distillation of seawater reverse osmosis brines, *Water Res.* 44 (18) (2010) 5260–5273.
- [7] F. Edwie, T.S. Chung, Development of hollow fiber membranes for water and salt recovery from highly concentrated brine via direct contact membrane distillation and crystallization, *J. Memb. Sci.* s 421–422 (12) (2012) 111–123.
- [8] J. Ge, et al., Membrane fouling and wetting in a DCMD process for RO brine concentration, *Desalination* 344 (2014) 97–107.
- [9] M. Gryta, Fouling in direct contact membrane distillation process, *J. Memb. Sci.* 325 (1) (2008) 383–394.
- [10] L.D. Tijing, et al., Fouling and its control in membrane distillation—a review, *J. Memb. Sci.* 475 (2015) 215–244.
- [11] P. Zhang, et al., Scale reduction and cleaning techniques during direct contact membrane distillation of seawater reverse osmosis brine, *Desalination* 374 (2015) 20–30.
- [12] Q.M. Nguyen, S. Jeong, S. Lee, Characteristics of membrane foulants at different degrees of SWRO brine concentration by membrane distillation, *Desalination* 409 (2017) 7–20.
- [13] J.A. Sanmartino, et al., Treatment of reverse osmosis brine by direct contact membrane distillation: chemical pretreatment approach, *Desalination* 420 (2017) 79–90.
- [14] H. Ji, et al., Vacuum membrane distillation for deep seawater: experiments and theory, *Desalin. Water Treat.* 58 (2017) 344–350.
- [15] U. Dittscher, D. Woermann, G. Wiedner, Temperature polarization in membrane distillation of water using a porous hydrophobic membrane, *Zeitschrift für Elektrochemie, Berichte der Bunsengesellschaft für physikalische Chemie* 98 (8) (2010) 1056–1061.
- [16] L. MartíNez-DíEz, M.I. Vázquez-González, Temperature and concentration polarization in membrane distillation of aqueous salt solutions, *J. Memb. Sci.* 156 (2) (1999) 265–273.
- [17] J. Zhang, et al., Modelling of vacuum membrane distillation, *J. Memb. Sci.* 434 (2013) 1–9.
- [18] J.I. Mengual, M. Khayet, M.P. Godino, Heat and mass transfer in vacuum membrane distillation, *Int. J. Heat Mass Transf.* 47 (4) (2004) 865–875.
- [19] Z. Li, et al., Synergic effects of hydrophilic and hydrophobic nanoparticles on performance of nanocomposite distillation membranes: an experimental and numerical study, *Sep. Purif. Technol.* 202 (2018) 45–58.
- [20] Y. Yang, et al., The heat and mass transfer of vacuum membrane distillation: effect of active layer morphology with and without support material, *Sep. Purif. Technol.* 164 (2016) 56–62.
- [21] R. Zhou, et al., Effects of multi-walled carbon nanotubes (MWCNTs) and integrated MWCNTs/SiO₂ nano-additives on PVDF polymeric membranes for vacuum membrane distillation, *Sep. Purif. Technol.* 217 (2019) 154–163.
- [22] M. Qtaishat, et al., Heat and mass transfer analysis in direct contact membrane distillation, *Desalination* 219 (1–3) (2008) 272–292.
- [23] A.S. Alsaadi, et al., Experimental and theoretical analyses of temperature polarization effect in vacuum membrane distillation, *J. Memb. Sci.* 471 (6) (2014) 138–148.
- [24] M.H. Sharqawy, J.H.L. V, S.M. Zubair, Thermophysical properties of seawater: a review of existing correlations and data, *Desalin. Water Treat.* 16 (1–3) (2010) 354–380.
- [25] B.K. Pramanik, et al., A critical review of membrane crystallization for the purification of water and recovery of minerals, *Rev. Environ. Sci. Biotechnol.* 15 (3) (2016) 411–439.
- [26] H. Zhu, et al., Preparation and properties of PTFE hollow fiber membranes for desalination through vacuum membrane distillation, *J. Memb. Sci.* 446 (1) (2013) 145–153.
- [27] H.J. Hwang, et al., Direct contact membrane distillation (DCMD): experimental study on the commercial PTFE membrane and modeling, *J. Memb. Sci.* 371 (1–2) (2011) 90–98.
- [28] S. Adnan, et al., Commercial PTFE membranes for membrane distillation application: effect of microstructure and support material, *Desalination* 284 (2) (2012) 297–308.
- [29] E. Drioli, A. Ali, F. Macedonio, Membrane distillation: recent developments and perspectives, *Desalination* 356 (2015) 56–84.
- [30] J. Jia, G. Kang, Y. Cao, Effect of Stretching Parameters on Structure and Properties of Polytetrafluoroethylene Hollow-Fiber Membranes, *Chem. Eng. Technol.* 39 (5) (2016) 935–944.
- [31] J. Jia, et al., Sintering process investigation during polytetrafluoroethylene hollow fibre membrane fabrication by extrusion method, *High Perform. Polym.* 29 (1) (2017) p. 095400831666940.
- [32] X. Jian, Z.L. Xu, Poly(vinyl chloride) (PVC) hollow fiber ultrafiltration membranes prepared from PVC/additives/solvent, *J. Memb. Sci.* 208 (1) (2002) 203–212.
- [33] H. Yasuda, J.T. Tsai, Pore size of microporous polymer membranes, *J. Appl. Polym.*

- Sci. 18 (3) (2010) 805–819.
- [34] J.A. Otero, et al., Three independent ways to obtain information on pore size distributions of nanofiltration membranes, *J. Memb. Sci.* 309 (1) (2008) 17–27.
- [35] M.C. García-Payo, M. Essalhi, M. Khayet, Effects of PVDF-HFP concentration on membrane distillation performance and structural morphology of hollow fiber membranes, *J. Memb. Sci.* 347 (1–2) (2010) 209–219.
- [36] S. Srisurichan, R. Jiraratananon, A.G. Fane, Humic acid fouling in the membrane distillation process, *Desalination* 174 (1) (2005) 63–72.
- [37] Y. Choi, et al., Fractional-submerged membrane distillation crystallizer (F-SMDC) for treatment of high salinity solution, *Desalination* (2018).
- [38] L.D. Nghiem, T. Cath, A scaling mitigation approach during direct contact membrane distillation, *Sep. Purif. Technol.* 80 (2) (2011) 315–322.
- [39] D. Qu, et al., Study on concentrating primary reverse osmosis retentate by direct contact membrane distillation, *Desalination* 247 (1) (2009) 540–550.
- [40] G. Naidu, et al., Application of vacuum membrane distillation for small scale drinking water production, *Desalination* 354 (354) (2014) 53–61.
- [41] J.J.D. Yoreo, P.G. Vekilov, Principles of crystal nucleation and growth, *Rev. Mineral. Geochem.* 54 (1) (2003) 57–93.
- [42] F. Edwie, T.S. Chung, Development of simultaneous membrane distillation–crystallization (SMDC) technology for treatment of saturated brine, *Chem. Eng. Sci.* 98 (29) (2013) 160–172.
- [43] A. Ferreira, et al., Using image analysis to look into the effect of impurity concentration in NaCl crystallization, *Chem. Eng. Res. Des.* 83 (4) (2005) 331–338.